Journal of Hydroscience and Hydraulic Engineering
Vol. 30, No.2 November, 2012, 49-64

FLOW RESISTANCE AND SEDIMENT TRANSPORT RATE IN ALLUVIAL STREAMS WITH SEDIMENTARY DUNES

By

Hiroshi Miwa

Department of Civil Engineering, Maizuru National College of Technology, Maizuru, Kyoto, Japan

and

Atsuyuki Daido

East Asian Office of Technology, Fushimi-ku, Kyoto, Japan

SYNOPSIS

Prediction methods of flow resistance and bed-load transport rate in alluvial streams with sedimentary dunes under lower flow regime are proposed in this study. At first, a skin friction equation is derived by integrating the grain-roughness shear stress distribution equation on the dune surface. Next, an equation of flow resistance based on equations of skin friction and form drag is proposed. The flow resistance equation is verified by estimating the mean depth of flow over dunes. An equation of effective tractive force is also proposed, and then the difference between the skin friction and the effective tractive force is discussed. The reach averaged bed-load transport rate can be calculated reasonably by the Meyer Peter & Müller's equation by using the proposed effective tractive force equation and estimated mean flow depth. The proposed method can predict the mean flow depth, mean length and height of dunes, as well as bed-load transport rate by providing water discharge, bed slope and grain size as input variables. The method which we propose also clarifies that the ratio of the form drag and the skin friction to the total shear stress is different in uniform and non-uniform sediment beds.

INTRODUCTION

Sand waves such as dunes strongly influence flow resistance. In order to estimate the bed-load transport rates adequately, an evaluation method of flow resistance including the effects of sand waves is indispensable. Many studies have been conducted on flow resistance in alluvial streams with sand waves, and they can be categorized into two groups: inductive method (e.g. Einstein and Barbarossa (1), Engelund (2), (3), Kishi and Kuroki (4)) and deductive methods (e.g. Yalin (5), Vanoni and Hwang (6), Kikkawa and Ishikawa (7)). The inductive method is used to formulate the relationship between the flow resistance and hydraulic parameters obtained by dimensional analysis on the basis of a large number of measurement data. The deductive method is used to describe the flow resistance on the basis of the dynamic law considering the sand wave geometry (wavelength and height). The former is a very simple and practical method because the sand wave geometry does not appear in the flow resistance equation explicitly.

But, this method cannot describe the mechanism of flow resistance. As for the latter, the mechanism of flow resistance is more distinct, and it can be applied to discussions of sediment transport phenomena. However, even this method requires sand wave geometry beforehand. Since sand wave geometry also depends on the flow resistance, it has to be taken into account as an unknown parameter in the flow resistance estimation. However, so far no research has been conducted on these matters.

Theoretical analyses of flow resistance estimation and numerical simulations of sand wave evolution have been conducted in recent years. As for the hysteresis, which is analogous to the multiple-valued relations between the Shields stress and the grain-roughness Shields stress, in the transition process of dune formation, Yamaguchi and Izumi (8) performed a weakly nonlinear analysis in order to provide a theoretical explanation for the hysteresis. Onda and Hosoda (9) tried to reproduce the dune formation and development by means of the numerical simulation, and to estimate the velocity coefficient. They also compared their reproduction and estimation results with results computed by the former methods. But, the flow separation zone was not considered in their simulation. Giri and Shimizu (10) conducted a simulation of the dune formation and migration process by considering the flow separation zone formation. Giri and Shimizu (11) also reproduced an increase in flow depth along with the dune formation and development by means of the numerical simulation. Sekine (12) tried to reproduce the sand wave formation process on the basis of the momentum equation of an individual sediment particle, and also discussed the step length of the particle. As mentioned above, many studies on numerical simulation of dunes have dealt mainly with their shape and migration properties, and have hardly discussed flow resistance and its mechanism.

This paper deals with the flow resistance estimation method that can predict dune geometry, and discusses the prediction of sediment transport system on the basis of the estimation method. At first, a skin friction equation is derived by integrating the grain-roughness shear stress distribution equation on the dune surface. And then, the skin frictions calculated by the derived equation are compared with those by the former equations. A flow resistance equation based on the skin friction and form drag equations will be proposed next, and the proposed equation is verified with estimations of mean depth of flow over dunes. An equation of effective tractive force is also proposed, and then the difference between the skin friction and the effective tractive force is presented. After that, the reach averaged bed-load transport rate will be calculated using the proposed effective tractive force equation. The ratio of the skin friction and the form drag to the total shear stress in uniform and non-uniform sediment beds is investigated by the proposed method.

EXPERIMENTAL SETUP

Movable bed and fixed bed experiments were conducted in a straight rectangular open channel, 6 m long, 0.2 m wide. Two kinds of nearly uniform sediment were used in experiments for movable bed. Figure 1 shows their grain

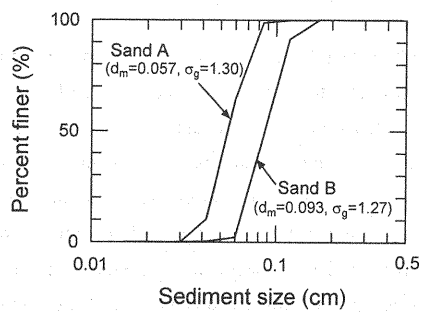

Fig. 1 Grain size distributions of the sediments used

size distributions. Sand A has a mean grain diameter d_m of 0.057 cm, a geometric standard deviation σ_g ($=\sqrt{d_{84}/d_{16}}$, in which d_{84} and d_{16} are the grain sizes for which 84 % and 16 % of the sediment is finer respectively) of 1.30 and a specific gravity σ_s of 2.65. Sand B has d_m = 0.093 cm, σ_g = 1.27 and σ_s = 2.65.

The sand bed was flattened with a scraper, and was set to a slope of 0.0025 (1/400) before commencing the experiments. In these experiments, dunes were allowed to develop under the prescribed water discharge. The sediment was externally fed into the flow at the upstream end of the channel in order to keep the average bed level constant. After dunes had fully developed, water surface elevations were measured at intervals of 10 cm in the flow direction just before stopping the water supply, using a point gauge. Bed elevations were measured at the same intervals, and in addition at the troughs and crests along three lines (2 cm from each side wall and the center of the channel) after stopping the water supply. Temporal and spatial variations in the water surface and bed configurations were measured, and the mean flow depth was obtained. Lengths and heights of dunes were measured by the trough-to-trough method (13). The bed-load transport rate was measured by the catching the sediment during the passing time of one dune-length at the downstream end of the channel. The experimental conditions for the movable bed experiments are listed in *Table 1* in which each value is in a stable state of the bed. In the table, symbols are defined as follows: q_w = water discharge per unit width of the channel; h = mean flow depth; I_e = energy slope (between 1 and 4 m from the downstream end of the channel); F_r = Froude number; u_* = shear velocity ($=\sqrt{gR_bI_e}$, in which g is the acceleration of gravity; R_b is the hydraulic radius whose wall effect was removed by Einstein's method (14)); q_B = volumetric bed-load transport rate per unit width of the channel; R_{e*} = sediment Reynolds number ($= u_*d_m/\nu$, in which ν is the kinematic viscosity of water); L = mean dune length; and H = mean dune height. In the each experiment, the stable state of the bed means that the dune geometry did not change temporally and that the bed-load transport rate and the sediment feeding rate were almost the same.

As for the fixed bed experiment, two kinds of dune models were used. One model had a dune length L_{mod} of 40 cm and a dune height H_{mod} of 1 cm, the other model had L_{mod} = 40 cm and H_{mod} =2 cm. Each model had a surface roughness of approximately 0.06 cm and a lee side with the elevation angle of 45 degrees. A dune bed was formed by arranging the model to the channel bed, and set to the prescribed slope before the experiments. Bed elevations were also measured at intervals of 10 cm in the flow direction, and at troughs and crests along the center line of the channel. In the experiment, water surface elevations were measured at the same intervals along the center line of the channel. The experimental conditions for the fixed bed experiments are listed in Table 2.

Table 1 Experimental conditions for movable bed

Run No.	d_m (cm)	q_w (cm^2/sec)	h (cm)	I_e ($\times 10^{-3}$)	F_r	u_* (cm/sec)	q_B ($\times 10^{-2}$ cm^2/sec)	R_{e*}	L (cm)	H (cm)
U-1A	0.057	350	9.6	2.11	0.38	3.39	3.07	22.4	46.5	1.6
U-1B	0.057	350	9.3	2.79	0.39	4.54	4.49	25.9	64.3	2.0
U-1C	0.057	350	10.3	2.40	0.34	4.45	3.17	25.4	45.7	1.8
U-2A	0.057	400	10.4	3.11	0.38	5.10	6.22	29.0	44.3	2.2
U-2B	0.057	400	10.0	3.23	0.40	5.07	8.38	28.9	49.0	2.1
U-2C	0.057	400	9.8	3.25	0.42	5.23	6.05	28.6	44.6	2.4
U-3A	0.093	450	9.8	2.21	0.47	3.84	8.66	35.7	34.9	1.2
U-3B	0.093	450	9.5	2.19	0.49	3.72	8.57	34.6	34.7	1.2
U-3C	0.093	450	9.8	2.34	0.47	3.99	11.10	37.1	33.7	1.2

Table 2 Experimental conditions for fixed bed

Run No.	q_w (cm^2/sec)	h (cm)	I_e ($\times 10^{-3}$)	F_r	u_* (cm/sec)	R_{e*}	L_{mod} (cm)	H_{mod} (cm)
I-1	250	6.6	2.41	0.47	3.51	20.0	40.0	1.0
I-2	300	7.6	2.29	0.46	3.60	20.5	40.0	1.0
I-3	350	9.0	2.34	0.42	3.98	22.7	40.0	1.0
II-3	250	8.8	2.02	0.31	3.83	21.8	40.0	2.0
II-4	250	7.2	3.03	0.42	4.22	24.1	40.0	2.0
II-5	350	9.7	2.49	0.37	4.37	24.9	40.0	2.0
II-6	350	9.2	2.48	0.40	4.18	23.8	40.0	2.0
II-7	400	10.3	2.56	0.39	4.51	25.7	40.0	2.0
II-8	400	10.1	2.50	0.40	4.37	24.9	40.0	2.0

EVALUATION OF SKIN FRICTION AND EFFECTIVE SHEAR STRESS

The boundary layer developed from the re-attachment point of flow over a dune is relatively thin compared with the flow depth, dune height and distance from the re-attachment point of flow. Therefore, the pressure variation in the boundary layer can be considered as small enough (7). Miwa and Daido (15) presented the following grain-roughness shear stress distribution equation based on the momentum equation of the boundary layer over dunes derived by Nakagawa et al. (16).

$$\frac{\tau(x)}{\rho u_m^2} = \Pi\left(\frac{h}{k_s}\right)^{-1}\left(\frac{x}{k_s}\right)^{\frac{3}{4}} \tag{1}$$

where

$$\Pi = \left(\frac{B}{A}\right)^2 C^{1/4}\ ;\ A = 8.94\ ;\ B = \frac{2}{2-\zeta}\left\{\xi(1-n\lambda)\right\}^{-1/2}\ ;\ C \cong A^2\left\{0.26 + \frac{\lambda}{(F_r B)^2}\right\};$$
$$n \equiv \frac{L_s}{H}\ ;\ \xi \equiv \frac{L}{h}\ ;\ \zeta \equiv \frac{H}{h}\ ;\ \lambda \equiv \frac{H}{L} \tag{2a-h}$$

here ρ = density of water; u_m = mean depth-averaged flow velocity; k_s = equivalent sand roughness; x = distance from re-attachment point of flow; F_r = Froude number; L_s = separation length of flow; and λ = dune steepness. In general (17) the value of n varies from 5 to 6, however, in this study it was set to 5.

Skin friction is defined as an integration of the grain-roughness shear stress distribution on the dune surface, as follows:

$$\tau' = \rho u_*'^2 = \frac{\cos\gamma}{L}\int_0^{(L-L_s)/\cos\gamma} \rho u_*(x)^2\, dx \tag{3}$$

where u_*' = grain-roughness shear velocity; γ = elevation angle of dune surface; and $u_*(x)$ = local shear velocity. Substituting Eq. 1 into Eq. 3, the skin friction is yielded as follows:

$$\tau' = \frac{4}{7}\Pi'\left(\frac{h}{k_s}\right)^{-1/4}\rho u_m^2 \tag{4}$$

where

$$\Pi' = \left(\frac{B'}{A}\right)^2 C^{1/4}\ ;\ B' = \frac{2}{2-\zeta}\xi^{-1/8}\left(1-n\lambda\right)^{3/8}\left(1+\lambda^2\right)^{3/16} \tag{5a,b}$$

Figure 2 shows the comparison between Eq. 4 and equations proposed by other researchers (Engelund (2), Kishi and Kuroki (4) and Yalin (5)) for estimating the skin friction. $k_s = 2d_m$ for movable beds and k_s = surface roughness of the dune model for fixed beds were adopted in Eq. 4. Suzuki et al. (13) and Guy et al.'s (18) experimental data are also plotted in the figure. Engelund's, and Kishi and Kuroki's equations do not include the dune length and dune height in their equations. The estimation results yielded by Engelund's, and Kishi and Kuroki's equations are similar to those by Eq. 4. Yalin's equation includes the wavelength and height as the hydraulic parameters, but they are used only for calculating the ratio of the skin friction to the total shear stress. His skin friction is determined by the logarithmic resistance law for a rough surface. Therefore, the structure of skin friction is not similar to Eq. 4. It can be seen that the results estimated by Yalin's equation are less than those by Eq. 4. The reason of this is not known. However, it was found that when Yalin's equation was applied to dunes, which was derived for ripples, the estimation results are relatively small compared with other researcher's equations. These former equations give the skin friction, which is evaluated in relation to the mean flow over dunes. Therefore, these equations can be regarded as the indirect evaluation methods. On the other hand, since the skin friction based on Eq. 4 is calculated by integrating the grain-roughness shear stress distribution along the dune surface, the interior structure of the skin friction is considered and, therefore its physical meaning becomes clear.

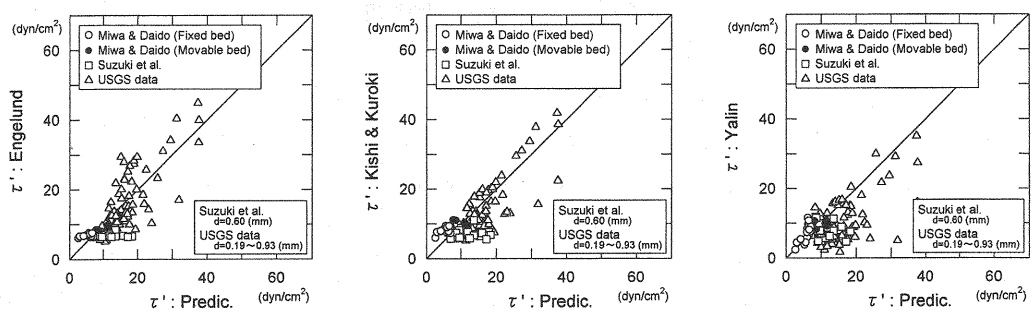

(a) Engelund (b) Kishi & Kuroki (c) Yalin

Fig. 2 Comparisons of evaluation results for skin friction τ' (d = grain diameter)

As indicated in Eq. 1, the grain-roughness shear stress gradually increases from the re-attachment point of flow on the dune surface. The sediment movement is possible in the area where grain-roughness shear stress is greater than the critical shear stress. Therefore, an effective tractive force, which contributes to sediment transport, can be defined as follows:

$$\tau_e = \frac{\cos\gamma}{L}\int_{x_c}^{(L-L_s)/\cos\gamma}\rho u_*(x)^2\,dx \tag{6}$$

where x_c denotes the location where $u_*(x)$ equals to u_{*c}, which is a critical shear velocity and can be evaluated with Iwagaki formulation (19). Then, x_c can be expressed from Eq.1 as

$$\frac{x_c}{h} = \Pi^{-4/3}\left(\frac{h}{k_s}\right)^{1/3}\left(\frac{u_{*c}^2}{u_m^2}\right)^{4/3} \tag{7}$$

Using Eqs. 6 and 7, the relationship between τ_e and τ' is yielded as follows:

$$\frac{\tau_e}{\tau'} = 1 - \Pi''^{-7/3}\left(\frac{h}{k_s}\right)^{7/12}\left(\frac{u_{*c}^2}{u_m^2}\right)^{7/3} \tag{8}$$

where

$$\Pi'' = \left(\frac{B''}{A}\right)^2 C^{1/4}\ ;\ B'' = \frac{2}{2-\zeta}\xi^{-1/8}(1-n\lambda)^{-1/8}\left(1+\lambda^2\right)^{3/16} \tag{9a,b}$$

The second term of the right side of Eq. 8 describes the reduction rate of τ_e to τ'. Figure 3 shows the relationship between τ_e/τ' and the Shields stress τ_* for the experiments in Table 1 and of Suzuki et al. (13), Guy et al. (18) and Ueno (20). When τ_* is larger than about 0.08, the values of τ_e/τ' are larger than 0.97, in which case τ_e can be considered to be equal to τ'. However, since the values of τ_e/τ' decrease rapidly along with the decrease of τ_* from 0.08, τ_e cannot always be considered equal to τ'. Therefore, the effective tractive force for bed-load transport calculation should be estimated by using Eq. 6.

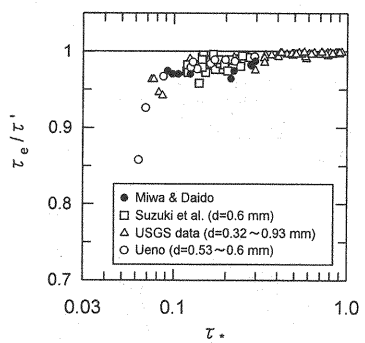

Fig. 3 Relationship between ratio of effective tractive force τ_e to skin friction τ' and Shields stress τ_*

RESISTANCE LAW AND ITS STRUCTURE

Hydraulic resistance of flow over dunes mainly consists of the skin friction and the form drag. The former is caused by grain-roughness and the latter is caused by the pressure imbalance between the upper and lower phases of an individual dune. In general, the total shear stress is expressed as

$$\tau = \tau' + \tau'' \tag{10}$$

where τ'' = form drag. Kikkawa and Ishikawa (7) proposed the following form drag equation by using drag

coefficient C_D.

$$\tau'' = \frac{1}{2} C_D \Lambda \rho u_m^2 \tag{11}$$

where

$$C_D = \frac{4(1-4\lambda)(2+\zeta)}{(2-\zeta)^2\{2+(1-8\lambda)\zeta\}}\left\{\frac{2(1-4\lambda)\zeta}{2+(1-8\lambda)\zeta}+0.13\right\};\ \Lambda = \frac{\lambda}{1+\zeta/2} \tag{12a,b}$$

By substituting Eqs. 4 and 11 into Eq. 10, the flow resistance equation has yielded as follows:

$$\frac{u_m}{u_*} = \left\{\frac{4}{7}\Pi'\left(\frac{h}{k_s}\right)^{-1/4} + \frac{1}{2}C_D\Lambda\right\}^{-1/2} \tag{13}$$

Equation 13 is able to calculate the mean flow depth when water discharge, bed slope, grain size and dune length and height are given. Figure 4 shows the comparison of calculated mean flow depths with measured ones using some other researchers' experiments. The calculated results show a slight overestimation, however, the accuracy may be considered to be sufficient.

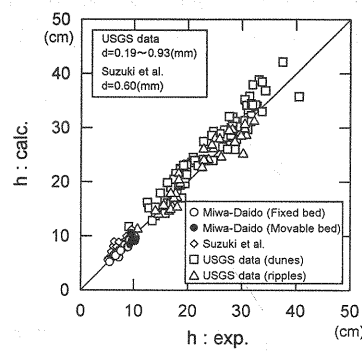

Fig. 4 Comparison of calculated mean flow depths h with experimental ones

As for the streams with dunes, it is important to clarify the relationship between the total shear stress τ and skin friction τ'. Engelund (2), (3) showed that the Shields stress τ_* is a function of just the grain-roughness Shields stress τ_*' on the basis of his similarity hypothesis. Kishi and Kuroki (4) found that τ_* relates to not only τ_*' but also the relative depth h/d (flow depth to grain diameter ratio) by classifying a large number of experimental data on bed forms, and proposed their functional relationship. Equation 4 shows that the skin friction is a function of h/k_s. Yalin and Karahan (21) found that the dune steepness depends on τ_* and h/d. From these two facts, it is easy to deduce that τ_*' varies with h/d too. Therefore, Kishi and Kuroki's approach mentioned above is very important. However, their proposal may not always be sufficient because the evaluation of flow resistance does include the dune geometry. Since the flow resistance of streams with dunes strongly depends on the dune geometry, a functional relationship considering geometrical properties of dunes needs to be discussed. Therefore, the relationship among τ_*, τ_*' and h/d will be discussed hereinafter by considering dune length and height.

By combining Eq. 13 with Eq. 4, the relationship between τ_* and τ_*' is obtained as follows:

$$\tau_* = \left\{1 + \frac{7}{8}\frac{C_D \Lambda}{\Pi'}\left(\frac{h}{k_s}\right)^{1/4}\right\}\tau_*' \tag{14}$$

where Π', C_D and Λ are parameters that depend on the dune geometry. If the dune length and height can be formulated by τ_* and h/d that consist of external variables such as grain size, flow depth and bed slope, the values of Π', C_D and Λ can also be calculated from the external variables. Therefore, in order to evaluate the relationship among τ_*', τ_* and h/d, the dune steepness and dune length need to be estimated by using the hydraulic variables. As for the dune steepness, the following equation formulated by Yalin and Karahan (21) is applied in this study.

$$\lambda = 0.0127(\eta - 1)\exp\left(\frac{1-\eta}{\eta_m - 1}\right) \tag{15}$$

where $\eta = \tau_*/\tau_{*c}$; and τ_{*c} = critical Shields stress; η_m is the value of η at the condition of maximum dune steepness $\lambda_{\max}$, and is formulated as

$$\eta_m = 1 + \frac{e}{0.0127}\lambda_{\max} \tag{16}$$

where e = base of natural logarithm. Since Yalin and Karahan (21) presented the relationship between $\lambda_{\max}$ and h/d by the illustration, it is inconvenient to obtain the relationship numerically. The relationship can be expressed by the following equation, which is also shown in Fig. 5.

$$\lambda_{\max} = \begin{cases} -0.058 + 0.02\ln\left(\dfrac{h}{d}\right) & ; \quad \dfrac{h}{d} < 400 \\ 0.062 & ; \quad \dfrac{h}{d} \geq 400 \end{cases} \tag{17}$$

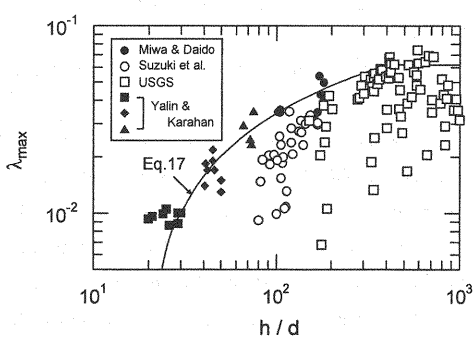

Fig. 5 Relationship between maximum dune steepness $\lambda_{\max}$ and relative depth h/d

Most of the experimental data provided by Yalin and Karahan in the figure show only the maximum dune steepness. However, other plotted values in the figure (obtained by other researchers) include all the data. It can also be seen that only the plotted values which are close to the line representing Eq. 17, show the maximum dune

steepness. Figure 6 shows the comparison of the measured data and those obtained from Eq. 15 by using Eq. 17. As seen from this figure, the fitting is quite good.

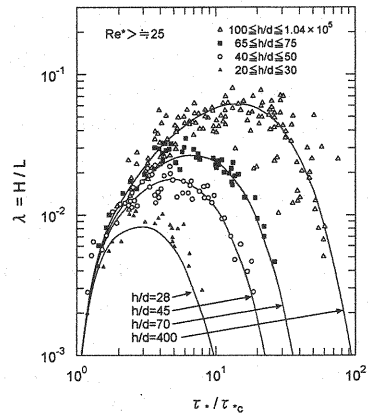

Fig. 6 Verification of Eq. 15 relating to maximum dune steepness λ_{max}

As for the dune length, the following relation described by Yalin (22) is applied.

$$L = \xi h \tag{18}$$

In general the value of ξ varies from 4 to 6, however, in this study it was set to 5.

This study is concerned only with the dune regime, not the transition regime. Therefore, the dune geometry estimation by Eqs. 15-18 is valid only for the dune regime. Some criteria between the dune regime and the transition regime have been presented by other researchers. For example, for the stable dunes and the transition including the occurrence of antidunes, the following criterion by Kishi and Kuroki (4) can be applied:

$$\tau_* = 0.07\left(\frac{h}{d}\right)^{2/5} \tag{19}$$

Figure 7 shows the relationship among τ_*', τ_* and h/d. The plotted values show the relationship between τ_*' calculated from Eq. 4 and τ_* obtained from experiments, and the solid lines show Eq. 14 using Eqs. 15-18 in the dune regime. Eq. 14 shows that the relationship between τ_*' and τ_* varies by the h/d, and this could be confirmed from the experimental results. Engelund's relation for τ_* and τ_*' is represented by a broken line in the figure for comparison.

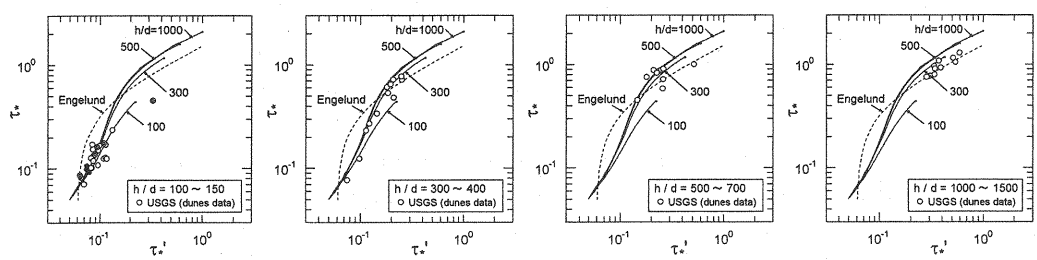

Fig. 7 Relationship between Shields stress τ_* and grain-roughness Shield stress τ_*'

The dune geometries such as dune length and height are unknown in the flow resistance prediction because they are dependent on variates, which are determined by the hydraulic conditions such as water discharge, flow depth, bed slope, etc. Therefore, the water depth can be predicted by combining Eq. 13 with Eqs. 15 and 18, and by using only water discharge, bed slope and grain size. The comparisons of predicted results with experimental values for mean flow depth are shown in Fig. 8. As compared to Fig. 4, which was obtained by using water discharge, bed slope, grain size, and dune length and height, the prediction accuracy of Fig. 8 is relatively low. However, the prediction method mentioned above is significant, because the resistance to flow can be predicted by only external conditions such as water discharge, bed slope and grain size. Figure 9 shows the comparison between predicted results and experimental values for dune length and height. As for the non-uniform sediment bed, the restriction effect of dune height due to grain sorting was introduced in the prediction of dune height as discussed later. While the predicted dune lengths are underestimated, the predicted dune heights show a good estimation.

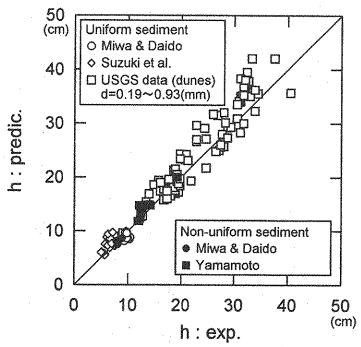

Fig. 8 Verification of prediction of mean flow depth h

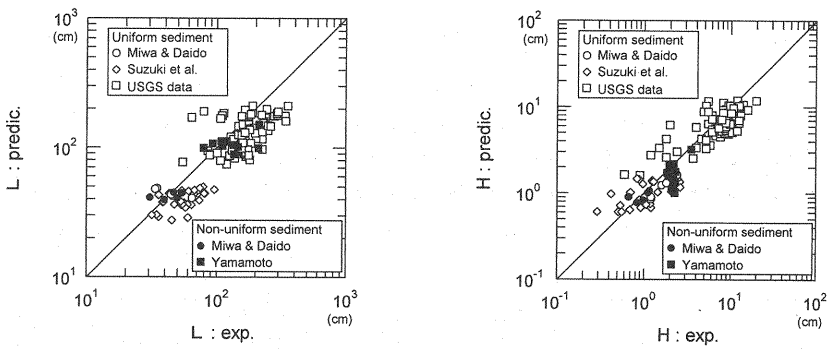

Fig. 9 Verification of prediction of mean dune length L and height H

Figure 4 also shows the accuracy level of Eq.13 on the flow depth prediction, when dune length and height are known. In contrast, the accuracy in Fig.8 is less than that in Fig.4 because in the former, calculations of dune length and height were needed in the flow depth prediction. However, the difference in accuracy between Fig.4 and Fig.8 is relatively small compared with the average accuracy of dune length (approximately 70 %). This means that the influence of the accuracy of dune length prediction to the flow depth prediction is rather small. Therefore, as for the

flow depth prediction, the accuracy in Fig. 9 is acceptable when the dune length and height are unknown. However, when higher accuracy of dune length prediction is required, e.g. dune transformation calculation, the value of α in Eq.18 should be expressed as a function of R_{e*} and h/d (e.g. Yalin (23)).

As mentioned above, the flow resistance in streams with dunes can be evaluated through the predictions of dune length and height. Consequently, the bed-load transport rate can also be predicted by using the effective tractive force. Figure 10 shows the bed-load transport rates obtained from the experiments against the effective Shields stress τ_{*e}, which is calculated from Eq. 8 using Eq. 4 and the predicted flow depths (Fig. 8). The solid lines in the figure show a modified version of the Meyer-Peter and Müller (24) formula

$$q_{B*} = \frac{q_B}{\sqrt{(\sigma/\rho - 1)gd^3}} = 8(\tau_{*e} - \tau_{*c})^{3/2} \tag{20}$$

where q_B = volumetric bed-load transport rate per unit width of the channel; and σ = density of bed material. Although the scatter of the measured data arranged by τ_{*e} are not always small, the line representing Eq. 20 shows the mean value of the measurement data. Therefore, we can conclude that dune geometry strongly influences the sediment transport rate. In order to estimate sediment transport rate properly, the effective tractive force has to be evaluated by considering effects of dune length and height explicitly. Figure 10 shows the result, which was estimated by incorporating the actual phenomena into the computation. From such perspective, findings of this study provide evidence that our prediction method is able to estimate sediment transport rate adequately.

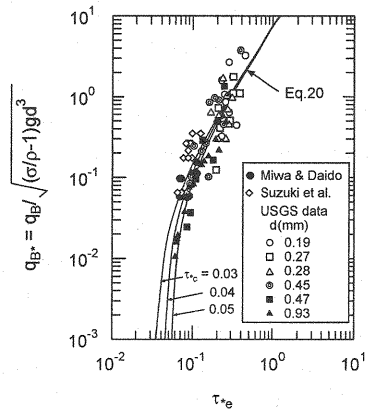

Fig. 10 Estimation of bed-load transport rate q_B using effective Shields stress τ_{*e}

All the discussions above are related to the uniform sediment beds. As for the non-uniform sediments beds with dunes, Miwa and Daido (15) found that the reference grain is coarse grain, whose diameter is approximately d_{90}. Therefore, in order to apply the above discussion of uniform sediment beds to non-uniform sediment beds, d_{90} has to be used instead of d_m. This means that the grain sorting effect on dune height is included in the calculation. Comparisons of predicted results and measured values for mean flow depth and dune length and height in the non-uniform sediment experiments of Miwa and Daido (15), and Yamamoto and Fukami (25) are also shown in Figs. 8 and 9. The prediction accuracies for the non-uniform sediment are found to be the same as the uniform sediment experiments. Figure 11 shows the comparison of the predicted results with the experimental values for the total shear stress τ in the uniform and non-uniform sediment experiments of Miwa and Daido (15), Ueno (20), and Yamamoto and Fukami (25). Each predicted value is shown by the summation of the skin friction given by Eq. 4 and the form drag

given by Eq. 11. The amounts of skin friction τ' and form drag τ'' are also indicated in the figure. The ratio of the form drag to the total drag is more than 1/2 in uniform sediment beds, whereas it is 1/4 to 1/3 in non-uniform sediment beds. There is a big difference between both beds. This reason for this is that the dune development is associated with the grain sorting in non-uniform sediment beds, and that the coarse grain fraction plays a role that restrains the dune height development (15). Therefore, the sediment transport rate in non-uniform sediment beds may be larger than that in uniform sediment beds under the same total shear stress condition.

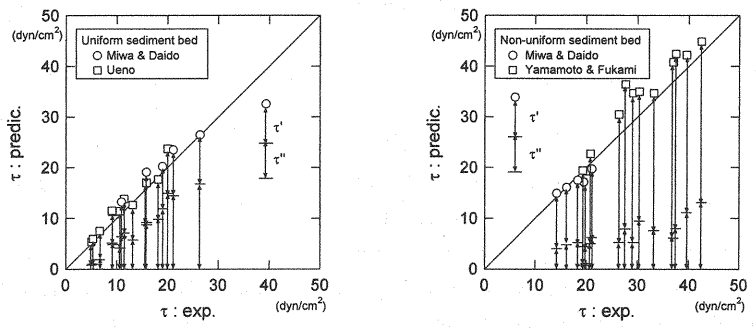

(a) Uniform sediment bed (b) Non-uniform sediment bed

Fig. 11 Predictions of total shear stress τ, and amount of skin friction τ' and form drag τ''

CONCLUSIONS

In this paper, we examined the flow resistance estimation method which could predict dune geometry in lower flow regime, and discussed the prediction of sediment transport system on the basis of the proposed method. The results may be summarized as follows:

1. The skin friction equation was derived by integrating the grain-roughness shear stress distribution on the dune surface. The skin friction calculated by this equation has a clear physical meaning and also reflects its interior structure clearly. The definition and equation of the effective tractive force were proposed, and the difference between the skin friction and the effective tractive force was presented. The effective tractive force can be considered equal to the skin friction at the larger values of the Shields stress, whereas they cannot be considered to be the same any longer at the smaller values of the Shields stress.

2. The equation of flow resistance was proposed on the basis of the equations of skin friction and form drag. The flow resistance equation is verified by estimating the mean flow depth over dunes. The relationship between the Shields stress and the grain-roughness Shields stress was formulated by considering the effects of the dune geometry.

3. The mean flow depth and dune length and height were predicted by using the water discharge, bed slope and grain size in the flow resistance equation combining dune steepness and dune length equations. The bed-load transport rate was also calculated by using the predicted effective tractive force. The predicted results were verified through the measured data.

4. The ratio of the form drag to the total drag is more than 1/2 in uniform sediment beds, whereas it is 1/4 to 1/3 in non-uniform sediment beds. It was found that there is a large difference between both beds. This reason for this is due to the fact that the dunes develop with grain sorting in non-uniform sediment beds, and coarse grain fraction plays an important role in restraining the dune height development.

In this study, we proposed a flow resistance estimation method under steady flow conditions in a dune regime.

By introducing the time evolution equations for dune length and height (e.g. Nakagawa et al. (26)) into the calculation, the proposed method can be applied to dune transformation process under unsteady flow conditions. However, it should be noted that the method is not always valid for unsteady phenomena in the transition regime. Extension of the method to the transition regime will be considered in the future research.

REFERENCES

1. Einstein, H. A. and Barbarossa, N.L. : River channel roughness, *Transactions of ASCE*, Vol.117, Paper No.2528, pp.1121-1132, 1952.
2. Engelund, F. : Hydraulic resistance of alluvial streams, *Jour. Hydraulics Division*, Vol.92, No.HY2, ASCE, pp.315-326, 1966.
3. Engelund, F. : Closure to discussion of hydraulic resistance of alluvial streams, *Jour. Hydraulics Division*, Vol.93, No.HY4, ASCE, pp.287-296, 1967.
4. Kishi, T. and Kuroki, M. : Bed form and resistance to flow in erodible-bed channels (I) -Hydraulic relations for flow over sand waves-, *Research Reports*, Faculty of Engineering, Hokkaido University, No. 67, pp.1-23, 1972 (in Japanese).
5. Yalin, M.S. : On the average velocity of flow over a movable bed, *La Houille Blanche*, No.1, pp.45-51, 1964.
6. Vanoni, V.A. and Hwang, L.S. : Relation between bed forms and friction in streams, *Journal of Hydraulics Division*, Vol.93, No.HY3, ASCE, pp.121-144, 1967.
7. Kikkawa, H. and Ishikawa, T. : Hydraulic resistance of streams over dunes and ripples, *Proceedings of JSCE*, No.281, pp.55-63, 1979 (in Japanese).
8. Yamaguchi, S. and Izumi, N. : Subcritical bifurcation observed in the transition between dune and flat bed regimes, *Journal of Hydraulic, Coastal and Environmental Engineering*, No.740/II-64, JSCE, pp.75-94, 2003 (in Japanese).
9. Onda, S. and Hosoda, T. : Numerical simulation on development process of dunes and flow resistance, *Annual Journal of Hydraulic Engineering*, Vol. 48, JSCE, pp.973-978, 2004 (in Japanese).
10. Giri, S. and Shimizu, Y. : Numerical computation of sand dune migration with free surface flow, *Water Resources Research*, Vol.42, W10422, 2006.
11. Giri, S. and Shimizu, Y. : Validation of a numerical model for flow and bedform dynamics, *Annual Journal of Hydraulic Engineering*, Vol. 51, JSCE, pp.139-144, 2007.
12. Sekine, M. : Numerical simulation of gravel bed deformation on the basis of particle motion analysis, *Annual Journal of Hydraulic Engineering*, Vol. 49, JSCE, pp.973-978, 2005 (in Japanese).
13. Suzuki, K., Michiue, M. and Iwagaki, K. : Study on the influence of channel width on the bed form, *Proceedings of the 25th Japanese Conference on Hydraulics*, JSCE, pp.35-40, 1981 (in Japanese).
14. Einstein, H. A. : Formulas for the transportation of bed load, *Transactions of ASCE*, Paper No.2410, pp.561-597, 1941.
15. Miwa, H. and Daido, A. : Sand wave development with sediment sorting, *Journal of Hydroscience and Hydraulic Engineering*, Vol.10, No.2, JSCE, pp.39-50, 1992.
16. Nakagawa, H., Tsujimoto, T., Murakami, S. and Mizuhashi, Y. : Spatial distribution of bed load transport rate over two-dimensional dunes, *Proceedings of the 28th Japanese Conference on Hydraulics*, JSCE, pp.735-741, 1984 (in Japanese).
17. Nakagawa, H. and Tsujimoto, T. : *Mechanics of Sediment Transport and Alluvial Hydraulics* (Idosho-Nagare no Suiri), Gihodo Shuppan, Chapter 8, 1986 (in Japanese).

18. Guy, H.P., Simons, D.B. and Richardson, E.V. : Summary of alluvial channel data from flume experiments, 1956-61, *Geological Survey Professional Paper*, 462-I, 1966.
19. Iwagaki,Y. : Hydrodynamic study on critical shear stress, *Proceedings of JSCE*, No.41, pp.1-21, 1956 (in Japanese).
20. Ueno, T. : On the regions of occurrence of ripples and dunes, *Proceedings of the 25th Japanese Conference on Hydraulics*, JSCE, pp.93-98, 1981 (in Japanese).
21. Yalin, M.S. and Karahan, E. : Steepness of sedimentary dunes, *Journal of Hydraulics Division*, Vol.105, No.HY4, ASCE, pp.381-392, 1979.
22. Yalin, M.S. : Geometrical properties of sand waves, *Journal of Hydraulics Division*, Vol.90, No.HY5, ASCE, pp.105-119, 1964.
23. Yalin, M.S. : *Mechanics of Sediment Transport*, 2nd edition, Pergamon Press, Oxford, 1977.
24. Meyer-Peter, E. and Müller, R. : Formulas for bed-load transport, *Proceedings of the 2nd IAHR Congress*, Stockholm, Sweden, pp.39-64, 1948.
25. Yamamoto, K. and Fukami, C. : Research note on mechanisms of sediment transport in rivers, *Technical note of Public Work Research Institute*, Ministry of Construction, No.1416, 1978 (in Japanese).
26. Nakagawa, H., Tsujimoto, T. and Takezuka, M. : Characteristics of unsteady flow with sand waves, *Proceedings of the 27th Japanese Conference on Hydraulics*, JSCE, pp.665-671, 1983 (in Japanese).

APPENDIX – NOTATION

The following symbols are used in this paper:

C_D = drag coefficient;

d = grain diameter;

d_m = mean grain diameter;

d_{84} = grain size for which 84 % of the sediment is finer;

d_{16} = grain size for which 16 % of the sediment is finer;

e = natural logarithm;

F_r = Froude number;

g = acceleration of gravity;

h = mean flow depth, measured from mean bed level;

H = mean dune height;

H_{mod} = dune height of model;

I_e = energy slope;

k_s = equivalent sand roughness;

L = mean dune length;

L_{mod} = dune length of model;

L_s = separation length of flow;

q_w = water discharge per unit width of the channel;

q_B = volumetric bed-load transport rate per unit width of the channel;

q_{B*} = dimensionless volumetric bed-load transport rate per unit width of the channel;

R_b = hydraulic radius whose wall effect was removed by Einstein's method (14);

R_{e*} = sediment Reynolds number (= $u_* d_m / \nu$);

u_m = mean depth-averaged flow velocity;

u_* = shear velocity (= $\sqrt{gR_b I_e}$);

$u_*(x)$ = local shear velocity;

u_{*c} = critical shear velocity;

u_*' = grain-roughness shear velocity (= $\sqrt{\tau'/\rho}$);

x = distance from re-attachment point of flow on dune surface;

x_c = location where $u_*(x)$ equals to u_{*c};

γ = elevation angle of dune surface;

η = ratio of τ_* to τ_{*c};

η_m = value of η at the condition of maximum dune steepness;

λ = dune steepness (= H/L);

λ_{max} = maximum dune steepness;

ν = kinematic viscosity of water;

ρ = density of water;

σ = density of bed material;

σ_g = geometric standard deviation (= $\sqrt{d_{84}/d_{16}}$);

σ_s = specific gravity of bed material;

τ = total shear stress;

$\tau(x)$ = local grain-roughness shear stress;

τ_e = effective tractive force;

τ_* = Shields stress;

τ' = skin friction;

τ'' = form drag;

τ_*' = grain-roughness Shields stress;

τ_{*c} = critical Shields stress; and

τ_{*e} = effective Shields stress.

(Received Aug, 24, 2011 ; revised May, 11, 2012)